Cramér-Rao Lower-Bound for Round-Trip Delay Ranging with Subcarrier-Interleaved OFDMA

Emanuel Staudinger, Siwei Zhang, and Armin Dammann

***Abstract*—In this work we propose an orthogonal frequency-division multiple access with subcarrier interleaving jointly with round-trip delay ranging. We formulate the transmission chain and specifically focus on deriving a multi-link Cramér-Rao lower-bound (CRLB). The resulting CRLB is thoroughly analyzed, relevant parameters are discussed and simulations with 3GPP-LTE system parameters are conducted. Sub-meter ranging precisions are predicted, and the suitability of our proposed concept for cooperative positioning of robotic swarms with high relative mobility is shown.**

I. Introduction

LOCATION information is vital for many applications, such as seamless pedestrian navigation in outdoor and indoor environments, or localizing elements of cyberphysical systems for surveillance and exploration. The diversity of current and future applications requiring location information demands diverse requirements with respect to accuracy and precision, update rate, robustness, complexity, and scalability of the used positioning technique. Current research primarily focuses on requirement aspects such as accuracy and precision. However, scalability, complexity, and even more important a high update rate of location information are of utmost importance for emerging technologies such as autonomous robotic swarms for exploration applications.

In this work we focus on a heterogeneous robotic swarm for exploration purposes as illustrated in Fig. 1. Autonomous robotic swarms are thought of to efficiently explore environments such as extraterrestrial places or human life endangering places on earth. An example is exploring the Martian valley system called Valles Marineris to find traces of water and life [1]. In [2], [3] the authors propose an example of exploration algorithms based on Gaussian processes, where as in [4] a more unified framework for robotic swarm exploration is presented. However, the swarm localization problem and also the intra-swarm communication aspect are considered to be solved, which is not the case. For consistency within the context of wireless communication and positioning we refer to individual swarm elements in Fig. 1 as users. Hence, the swarm depicted in Fig. 1 can be viewed as a more generalized cooperative wireless sensor network (WSN). Various localization techniques such as cooperative positioning including wireless infrastructure, or anchor-free localization in the infrastructure-free case exist to obtain the users' location [5]–[7]. Obtaining location information within a cooperative WSN requires the following four system entities: protocols for information exchange, channel access, ranging techniques, and signal modulation. All four system entities have an impact on scalability, complexity, update rate, robustness, accuracy and precision of the localization process. We are specifically interested in anchor-free localization with decentralized algorithms and explain necessary system entities and related work within the next paragraphs.

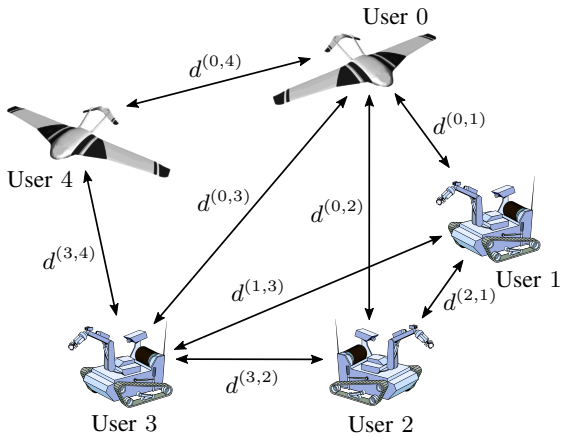

Fig. 1. A heterogeneous swarm with driving and flying swarm elements for exploration and surveillance. Arrows represent a wireless link for joint communication and ranging. The range between two swarm elements is denoted as $d^{(q,u)}$, with q as ranging initiator.

In [8] a self-organizing protocol for information exchange is presented, which can be used to exchange data from, e.g., distributed Bayesian localization estimators [7]. However, any scheduling aspect, the physical layer, and the wireless channel access itself are not considered. The channel access strategy is very important, as every user within the swarm should be able to communicate and range at least with its neighbors. Access collisions on the medium access control (MAC) layer lead to undesirable low ranging update rates particularly for WSNs with high relative mobility. Contention based MAC schemes, as for example used in ZigBee or WiFi based systems, suffer from multiple access interference resulting in unpredictable ranging update rates [9], [10]. Moreover, a channel access for all users cannot be guaranteed. Reservation based MAC schemes such as time division multiple access (TDMA) enable interference-free channel access for all users, but commonly require a dedicated master user to establish time slot reservation and scheduling [11]. A state of the art overview of various TDMA based MAC protocols is given in [9]. In [12] a location based TDMA MAC is introduced to reduce guard times between data packets for a network with large spatial dimensions. However, the presented MAC relies on a given global navigation satellite system (GNSS) to establish and preserve time slots. In example for extraterrestrial exploration, a GNSS

is not available. Without loss of generality, the amount of ranging links increases quadratically with the number of users $U_{\max}$ for a fully connected cooperative WSN. Any sequential but interference free channel access based on TDMA therefore results in the following key problem: the duration required to obtain all range estimates increases quadratically with $U_{\max}$ as well. Hence, scalability is low and additional positioning errors are introduced through quadratically increasing update delays [13]. As a consequence, such sequential ranging schemes result in a severely degraded localization performance, and are not applicable for cooperative WSNs with high relative mobility.

The third fundamental system entity is ranging, which is one method to infer location information compared to angle or connectivity based techniques. We refer to ranging as the estimation of the line-of-sight (LoS) distance between two users using radio signals, taking advantage of a distance dependent parameter of the same radio link. Distance dependent parameters are for example received signal strength (RSS), the propagation delay of the LoS signal, or the carrier phase. In this work we used propagation delay based ranging. Several methods to obtain distance information from a delay estimate exist, such as time-of-arrival (ToA), round-trip delay (RTD), or any other form of so called multi-way ToA ranging schemes [14]. ToA requires an accurate time synchronization among all users compared to RTD, which is hardly achievable within a WSN. The authors in [15], [16] present RTD based ranging techniques with orthogonal frequency division multiplex (OFDM) modulated signals particularly for space applications. [16] does not apply a distance dependent signal-to-noise ratio (SNR), and [15] relies on sub-optimal estimators for RTD estimation over additive white Gaussian noise (AWGN) channels without providing a lower bound for comparison. A related work is found in [17], where the authors present a new decentralized RTD ranging method with amplify and forward relays. Unfortunately, they do not provide a lower bound and their channel access scheme requires multiple time slots for which the clocks must not have any relative drift.

Our fourth and last system entity is signal modulation. Ultrawide bandwidth (UWB) based systems are commonly used in the localization community, which enable simple multipath mitigation without costly estimators but at the cost of a large bandwidth. Those ranging systems are typically realized as impulse-radio UWB, as chirp spread spectrum (CSS)-UWB, or as direct sequence spread spectrum (DSSS)-UWB [18]. In our work we use a multi-carrier signal based on OFDM, which is a widely used modulation technique in existing communication standards such as WiFi, WiMAX, or the 3rd Generation Partnership Project (3GPP) - Long Term Evolution (LTE) [10], [19], [20]. OFDM is currently the modulation technique of choice in communications to combat time-dispersive radio channels due to its low-complex channel equalization in frequency domain, but has not been exploited for ranging in such a degree as, e.g., CSS or DSSS in UWB systems [21]. Recent developments in radar, which can be related to propagation delay based ranging, incorporate OFDM to jointly estimate ranges and Doppler frequencies [22], [23]. A combination of OFDM and UWB for radar applications is presented in [24], [25], but the MAC itself it not considered and an open issue.

Localization performance depends on the relationship between the time spent to obtain range estimates between users and the relative mobility among those users. For example, very low range estimate updates rates will result in a large positioning error for users with high relative movement. The channel access scheme becomes the time-limiting factor. To overcome the drawback of quadratic link evaluation increase as described previously, we propose an orthogonal multiple access scheme based on OFDM subcarrier interleaving jointly with a decentralized TDMA reservation scheme and RTD ranging with amplify and forward relaying. We derive a new multi-link Cramér-Rao lower bound (CRLB) to predict the ranging precision of our proposition. CRLB evaluations with 3GPP-LTE physical layer (PHY) layer parameters show predicted sub-meter precisions. As a result, our proposition with its joint view on ranging precision and update rates is very suitable for cooperative WSNs with high relative mobility, such as robotic swarms for exploration.

This article is organized as follows: in Sec. II we recall our previous work on decentralized TDMA slot allocation, the principle of round-trip delay ranging and sparse OFDM subcarrier allocation, and show the concept of multiple access for ranging based on subcarrier interleaving. The multi-link transmission chain is described in Sec. III, followed by the CRLB derivation and discussion in Sec. IV. CRLB evaluation parameters and numerical results are presented and discussed in Sec. V, and we conclude in Sec. VI.

II. Ranging with Subcarrier-Interleaved OFDMA

A. Decentralized TDMA slot allocation

In [26] we presented a concept for decentralized TDMA slot allocation based on the pulse-coupled oscillator (PCO) principle. The PCO principle is biologically inspired and derived from the flashing of fireflies. It has been applied to decentrally synchronize WSNs and to establish a collision-free channel access [27]–[29]. In [26] we adapted this principle for our purposes. Hence, our reservation scheme does not require dedicated master users, and allows a flexible usage of time slots for new users joining an existing cooperative network. Furthermore, an interference-free channel access and deterministic channel access delays become possible. The upper illustration in Fig. 2 shows TDMA time slots. The amount of time slots is at least $U_{\max}$, or larger to allow for newly joining users. Within each time slot a user broadcasts a number of OFDM symbols, see the lower illustration in Fig. 2 as an example. The first two OFDM symbols are dedicated for frame synchronization (SYNC) to establish and maintain the decentralized TDMA reservation scheme. Two OFDM symbols are reserved for subcarrier-interleaved RTD (SI-RTD) ranging, and the remaining OFDM symbols can freely be used for data transmission, e.g., data required for the cooperative localization process, or scientific data from sensors.

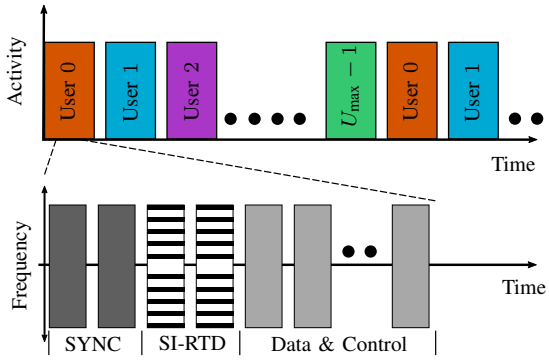

Fig. 2. TDMA slots decentrally assigned to different users (upper plot), and the OFDM framing within one time slot for broadcasting (lower plot). Each OFDM frame consists of OFDM symbols for frame synchronization (SYNC), ranging (SI-RTD), and additional OFDM symbols for data & control [26].

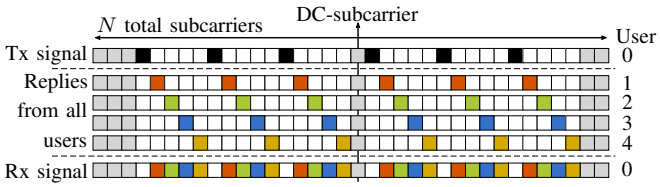

Fig. 3. Principle of subcarrier interleaving for RTD ranging in a cooperative network as shown in Fig. 1. Here, user 0 broadcasts a sparsely allocated signal with a specific, beneficial allocation for ranging. Each other user transparently relays the signal back and applies a unique subcarrier shift. User 0 receives a superimposed signal to obtain range estimates to all other users within one OFDM symbol. White boxes indicate unallocated subcarriers.

B. Transparent round-trip delay ranging

Our ranging technique is based on round-trip delay with transparent relaying, which we shortly recall next. The common problem of round-trip delay ranging, also known as two-way ranging, is its sensitivity to clock drifts between two users and the required large signal bandwidth to properly detect and time-stamp the received signal in environments with strong multipath [30], [31]. Clock drifts can be compensated at the high cost of multi-way ranging schemes, which inherently require multiple channel accesses and therefore increase the update delay [32], [33]. This particular clock drift problem can be fully avoided, once the user who receives a signal from the ranging initiator operates as transparent relay with amplify&forward relaying on the physical layer. In [34] and [35] we have experimentally proven this new scheme in various environments for single-link ranging, and obtained sub-meter accuracies and a very high ranging precision for two unsychronized users. However, single-link scenarios with two users have only been addressed theoretically and experimentally, and an extension for multiple users has been missing.

C. Sparse OFDM subcarrier allocation

Our concept of sparse subcarrier allocation for ranging in general has been proposed in [36]. The idea behind sparse subcarrier allocation is to only allocate few subcarriers of an OFDM symbol but distributed over the entire usable bandwidth, see the Tx signal in Fig. 3. A so called sparsity factor is introduced in [36] to steer the amount of allocated subcarriers. This allocation scheme can also be related to a specific scattered pilot structure used for channel estimation in, e.g., 3GPP-LTE, but our scheme generalizes the concept of scattered pilots [19], [21]. The key finding based on CRLBs was that we theoretically need only few allocated and power-normalized subcarriers distributed over the entire usable bandwidth to achieve the approximately same ranging precision, compared to allocating every subcarrier within the same bandwidth. In [36] we showed based on 3GPP-LTE OFDM parameters that we can use four subcarriers compared to 1200 within the $20\,\mathrm{MHz}$ bandwidth, to obtain the approximately same ranging precision. Naturally, we extended this sparse allocation scheme to subcarrier-interleaved orthogonal frequency division multiple access (OFDMA), which we describe next.

D. Subcarrier-interleaved OFDMA

Combining the three afore mentioned techniques namely decentralized TDMA, transparent RTD ranging, and sparse OFDM subcarrier allocation leads to our proposed subcarrier-interleaved OFDMA scheme. The key behind SI-RTD is as follows, assuming it's user 0's time slot: user 0 broadcasts a sparsely allocated OFDM signal based on theoretical findings from [36], see the transmit (Tx) signal representation in frequency domain in Fig. 3. The remaining users 1 to 4 are in a relaying mode because it's user 0's time slot. They receive this specific sparsely allocated signal and transparently forward the received signal with an additional, user specific subcarrier shift back to user 0 as ranging initiator, see Fig. 3.

The ranging initiator receives all replied signals simultaneously, and obtains a superimposed received signal from which the range to each user can be estimated. Subcarrier shifts must be unique and can be assigned dynamically when new users are joining the cooperative network during the decentralized TDMA, or a-priori for a maximum fixed number of users $U_{\max}$. Key benefits of SI-RTD are as follows: the ranging initiator in each TDMA slot can separate the users' replied signals in frequency domain with low complexity, as long as subcarrier orthogonality is preserved. Relaying users do not need to know the specific emitted ranging signal, as they only require knowledge about their unique subcarrier shift a-priori. Hence, the ranging initiator can adapt the sparsely allocated OFDM signal during runtime, e.g., additionally shaping the signal in frequency domain. The greatest benefit of SI-RTD is the linear link evaluation duration proportional to $U_{\max}$ compared to the quadratic duration increase for state of the art sequential channel access schemes as described in Sec. I. Let us affirm this with tangible numbers: we assume a TDMA slot duration of $0.4\,\mathrm{ms}$ and a maximum number of users of $U_{\max} = 30$. In the state of the art sequential case, we require $U_{\max}\cdot(U_{\max}-1)$ channel accesses to obtain all range estimates within the network and to communicate those range estimates. Hence, the overall update duration is $0.4\,\mathrm{ms}\cdot 30\cdot 29 = 0.348\,\mathrm{s}$, which is unfavorable for a heterogeneous network with higher relative mobility as depicted in Fig. 1. For SI-RTD we only require $0.4\,\mathrm{ms}\cdot 30 = 0.012\,\mathrm{s}$. A significant improvement compared to state of the art, as ranging is now performed

parallel compared to conventional schemes which perform sequential ranging.

Our concept of SI-RTD is closely related to OFDMA used within the communication community [37]. Within the OFDMA context, uplink is referred to a radio link from one user to a base station. In terms of OFDMA, SI-RTD directly relates to an interleaved carrier assignment scheme (CAS) for multiple distributed users in the uplink [37]. However, OFDMA is seldom used for uplink transmission in mass-market applications. Uplink synchronization among distributed users becomes challenging, and complex iterative receivers with interference cancellation are commonly used to achieve a sufficient communication performance. In some work within the uplink OFDMA context, ranging is not referred to distance estimation but rather to the initial access and sounding the uplink channel between the mobile user and a base station [38]–[40]. This fact can be misleading when existing literature is reviewed. For a fair comparison, challenges of SI-RTD for practical realizations should also be denoted: ranging performance will depend on carrier frequency offsets and Doppler frequency shifts in the same way as for uplink OFDMA. However, we are interested in the lower bound which serves as reference for further research. Besides the OFDMA context we also found a related work in the field of radar. In [41] the authors describe a new method for simultaneous polarimetric measurements, which exactly uses a sparsely allocated OFDM symbol with a sparsity factor of 2, but within a different context.

III. Multi-link transmission chain

We focus on a single TDMA slot, for which user 0 becomes the ranging initiator denoted as q. All remaining users 1 to $U_{\max-1}$ operate as transparent relays for the duration of the ranging signal, see Fig. 3. For compact notation we denote (u) as index for a specific transparent relay, with $u \neq q$. Fig. 4 shows the transmission chain for Cramér-Rao lower bound (CRLB) derivation in Sec. IV. The ranging initiator q transmits a in general complex time domain signal s_q with sampling time T_s. The forward link (FL) representing the mobile radio channel between q and the transparent relays u comprises two terms: the first term $h_{\text{FL}}^{(u)}$ denotes a channel impulse realization of a in general time-dispersive radio channel with a line-of-sight path propagation time of half the round-trip delay $\tau_{\text{RT}}^{(u)}$. The second term models the signal attenuation on the forward link as delay dependent path loss and is represented as amplitude factor

$$\Phi_{\text{FL}}^{(u)} = \sqrt{\left(2\pi f_{\text{c}} \tau_{\text{RT}}^{(u)}\right)^{-\gamma}}, \tag{1}$$

with γ as path loss exponent, f_{c} as carrier frequency, and $\tau_{\text{RT}}^{(u)}$ as the round-trip delay. The range $d^{(q,u)}$ between the ranging initiator q and a particular relay u is defined as

$$d^{(q,u)} = c_0 \frac{\tau_{\text{RT}}^{(u)}}{2}, \tag{2}$$

with c_0 as speed of light. Hence, the form of $\Phi_{\text{FL}}^{(u)}$ in (1). Each relaying user u receives the emitted signal, shifts it in frequency direction by an integer-multiple of the subcarrier spacing and transmits the signal back over the return link (RL) channel. Additive noise $z^{(u)}$ in each relay is modeled as white Gaussian distributed, with zero mean and variance $\sigma^{2,(u)}$. Amplification and subcarrier shifting is captured as a modulation term in time domain with discrete time index n as

$$\Psi^{(u)} = b^{(u)} e^{\mathrm{j}\phi^{(u)}} e^{-\mathrm{j}2\pi \frac{n}{N} \varrho^{(u)}}, \tag{3}$$

with $b^{(u)} \in \mathbb{R}$, $\left|b^{(u)}\right| > 1$ as known amplification factor for a particular relay u and $\phi^{(u)}$ as unknown phase offset. The unique normalized subcarrier shift per relay is represented by $\varrho^{(u)} \in \mathbb{Z}^+$, and N denotes the amount of subcarriers of an OFDM symbol. The OFDM symbol duration in time domain without the cyclic prefix is NT_s. Return link channels are modeled as their respective forward link channels. With an assumed channel reciprocity we can set $h_{\text{FL}}^{(u)} \equiv h_{\text{RL}}^{(u)}$ and $\Phi_{\text{FL}}^{(u)} \equiv \Phi_{\text{RL}}^{(u)}$. Furthermore, we also assume that individual FL and RL channels among individual relays u are uncorrelated. The ranging initiator receives the superposition of all relayed signals and adds white Gaussian distributed noise z_q with zero mean and variance σ_q^2. Transmitter and receiver within the ranging initiator are perfectly synchronized, which is simply achieved in the digital baseband. Thus, an estimated round-trip delay $\hat{\tau}_{\text{RT}}^{(u)}$ to each relay u based on the noisy received signal r_q can be retrieved. Taking the overall transmission chain into account, we find

$$\begin{aligned} r_q = & \underbrace{\sum_{u=1}^{U_{\max-1}} s_q * h_{\text{FL}}^{(u)} * h_{\text{RL}}^{(u)} \Phi_{\text{FL}}^{(u)} \Phi_{\text{RL}}^{(u)} \Psi^{(u)} +}_{\text{Signal term}} \\ & \underbrace{\sum_{u=1}^{U_{\max-1}} z^{(u)} * h_{\text{RL}}^{(u)} \Phi_{\text{RL}}^{(u)} \Psi^{(u)} + z_q,}_{\text{Noise term}} \end{aligned} \tag{4}$$

omitting any sampling indices for compact notation. We assumed that user 0 is the ranging initiator q and thus, the summation starts at user index $u = 1$ and ends with $U_{\max-1}$. The received signal r_q from (4) comprises two terms: a signal term and a noise term. The signal term consists of the sum of the initially transmitted signal s_q convoluted with the FL and RL channels to each particular relay and multiplied with FL and RL path losses, as well as the modulation term $\Psi^{(u)}$ with unique subcarrier shifts $\varrho^{(u)}$. An overall noise term comprises all relays' noise terms $z^{(u)}$ multiplied with the modulation term $\Psi^{(u)}$ and returned through the RL channel, as well as the ranging initiator's receiver noise z_q. A time-dispersive RL channel $h_{\text{RL}}^{(u)}$ will therefore result in a colored noise contribution $z^{(u)} * h_{\text{RL}}^{(u)}$ from each relay u.

Next, we derive the multi-link Cramér-Rao lower bound for modulation independent complex signals, as well as OFDM modulated signals.

IV. Multi-link CRLB

The Cramér-Rao lower bound (CRLB) is a common mathematical method to provide a lower bound on the variance of any unbiased estimator, and gives detailed insight how

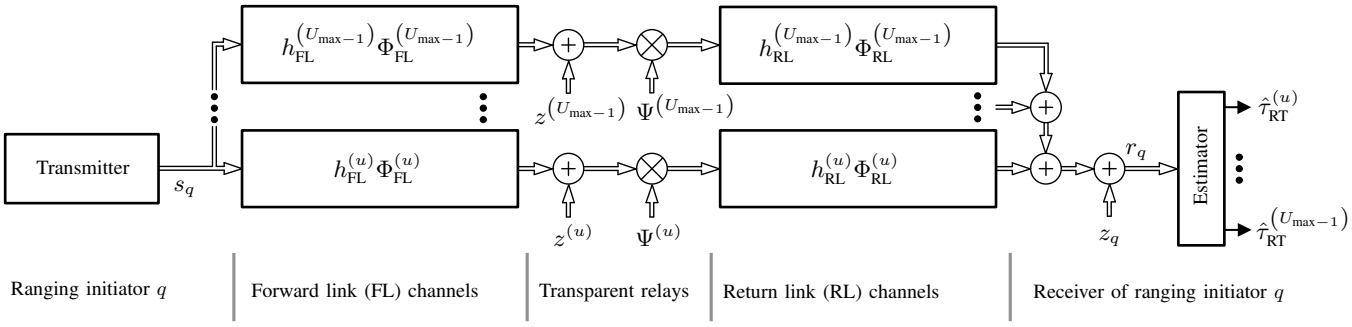

Fig. 4. Transmission chain for multi-link RTD ranging. Sampling indices n are omitted for compact notation.

system model parameters influence estimation performance [42, Chap. 3.1]. We refer to variance as the figure to quantify precision of an estimator. There exists no estimator for the same system model which can reach a precision lower than predicted by the CRLB. However, the CRLB does not necessarily reveal how to design such an estimator, and additionally, an estimation bias cannot be assessed with the CRLB [42, Chap. 3.2]. In our work, we investigate the precision of individual ranging links in a multi-link scenario as depicted in Fig. 1 and described in Sec. II, based on the denoted transmission chain in Fig. 4.

As in Sec. III we focus on a single TDMA slot, for which user 0 becomes the ranging initiator q. We are now interested in the variance of range estimates $d^{(u)} = d^{(q,u)}$, $q = 0$ and $u = 1 \dots U_{\max-1}$, but we can only observe an estimate of the round-trip delay denoted as $\hat{\tau}_{\mathrm{RT}}^{(u)}$. Given a vector of the sampled received signal $\mathbf{r}_q$ with N samples, and packing all individual true round-trip delays $\tau_{\mathrm{RT}}^{(u)}$ into a vector $\boldsymbol{\tau}_{\mathrm{RT}} = [\tau_{\mathrm{RT}}^{(1)}, \dots, \tau_{\mathrm{RT}}^{(U_{\max-1})}]^{\mathrm{T}}$ of length $U_{\max-1}$, we can define the variance of a particular range estimate $\hat{d}^{(u)}$ as

$$\begin{aligned} \mathrm{Var}\left\{\hat{d}^{(u)}\left(\mathbf{r}_q\right)\right\} &= \frac{c_0^2}{4}\mathrm{Var}\left\{\hat{\tau}_{\mathrm{RT}}^{(u)}\left(\mathbf{r}_q\right)\right\} \\ &= \frac{c_0^2}{4}\left[\mathrm{Cov}\left\{\hat{\boldsymbol{\tau}}_{\mathrm{RT}}\left(\mathbf{r}_q\right)\right\}\right]_{u,u}. \end{aligned} \tag{5}$$

The variance of a particular range estimate $\hat{d}^{(u)}$ is equal to the diagonal element $[\cdot]_{u,u}$ of the covariance matrix of estimated round trip delays to all relays u. Obtaining a lower bound on a particular range estimate requires the calculation of the Fisher information in the vector parameter case. A detailed fundamental derivation of the Fisher information in the vector parameter case can be found in [42, App. 3B]. The diagonal element $[\cdot]_{u,u}$ of the covariance matrix is lower bounded by the element $[\cdot]_{u,u}$ of the inverse of the Fisher information matrix

$$\left[\mathrm{Cov}\left\{\hat{\boldsymbol{\tau}}_{\mathrm{RT}}\left(\mathbf{r}_q\right)\right\}\right]_{u,u} \geq \left[\left[\mathrm{FIM}\left(\boldsymbol{\tau}_{\mathrm{RT}}\left(\mathbf{r}_q\right)\right)\right]^{-1}\right]_{u,u}, \tag{6}$$

with FIM as the Fisher information matrix. Individual FIM components are defined as

$$\left[\mathrm{FIM}\left(\boldsymbol{\tau}_{\mathrm{RT}}\left(\mathbf{r}_q\right)\right)\right]_{m,v} = -\mathbb{E}\left\{\frac{\partial^2}{\partial\tau_{\mathrm{RT}}^{(m)}\partial\tau_{\mathrm{RT}}^{(v)}}\ln p\left(\mathbf{r}_q|\boldsymbol{\tau}_{\mathrm{RT}}\right)\right\}, \tag{7}$$

with $\mathbb{E}$ as expectation value. Hence, we need to differentiate the conditional log-likelihood with respect to individual components m, v of interest and take the expectation value.

For further derivation we assume a non-time-dispersive channel with $h_{\mathrm{FL}}^{(u)} = h_{\mathrm{RL}}^{(u)} = \delta\left(t - \tau_{\mathrm{RT}}^{(u)}/2\right)$. Noise contributions $z^{(u)}$ and z_q represent Gaussian distributed noise with zero mean and constant power spectral density (PSD), are statistically independent and stationary processes. Taking the identity of the Dirac delta function δ into account we can reformulate (4) to

$$r_q = \sum_{u=1}^{U_{\max-1}} \underbrace{s_q\left(\tau_{\mathrm{RT}}^{(u)}\right)\Phi_{\mathrm{FL}}^{(u)}\Phi_{\mathrm{RL}}^{(u)}\Psi^{(u)}}_{\text{Signal term}} + \underbrace{z^{(u)}\Phi_{\mathrm{RL}}^{(u)}\Psi^{(u)} + z_q}_{\text{Noise term}}, \tag{8}$$

as the statistics of the delayed noise $z^{(u)}$ does not change.

Before we can combine the overall noise term in (8) into a single noise variable, we need to have a closer look at $\Phi_{\mathrm{RL}}^{(u)}$ and $\Psi^{(u)}$. The return link path loss $\Phi_{\mathrm{RL}}^{(u)}$ represents a delay dependent multiplicative value. As a consequence, the noise variance will scale with the path loss but the zero mean and constant PSD property are not affected. The modulation term $\Psi^{(u)}$ contains the relay gain $b^{(u)}$, which scales the noise variance again. However, the subcarrier shift is of interest: a particular subcarrier shift $\varrho^{(u)}$ in the digital signal processing domain always results in aliasing, as frequency components at the spectrum's edge are cyclically shifted back at the other spectrum's side. As long as the noise PSD is constant over the entire bandwidth, it will remain constant after subcarrier shifting. This condition requires a match between the relay's analog bandwidth of the receiver's front-end and the sampling rate within the receiver. Sampling at the Nyquist sampling rate fulfills this condition, but oversampling at the relay's receiver does not. We assume sampling at the Nyquist sampling rate and can therefore combine the sum of noise terms in (8) into a variable z_{RT} with noise variance

$$\begin{aligned} \sigma_{\mathrm{RT}}^2 &= \mathrm{Var}\left\{\sum_{u=1}^{U_{\max-1}} z^{(u)}\Phi_{\mathrm{RL}}^{(u)}\Psi^{(u)} + z_q\right\} \\ &= \sigma_q^2 + \sum_{u=1}^{U_{\max-1}} \sigma^{2,(u)}b^{2,(u)}\Phi_{\mathrm{RL}}^{2,(u)}, \end{aligned} \tag{9}$$

with $b^{2,(u)}$ and $\Phi_{\text{RL}}^{2,(u)}$ as the respective squared relay gain and return link path loss from each relay u.

Based on (8) and (9) the conditional probability function of the received signal $\mathbf{r}_q$ required for (7) is found as

$$p\left(\mathbf{r}_q|\boldsymbol{\tau}_{\text{RT}}\right) = \frac{1}{\left(\pi\sigma_{\text{RT}}^2\right)^N} e^{\sigma_{\text{RT}}^{-2}\sum_{n=0}^{N-1}\left|r_{q_n}-\sum_{u=1}^{U_{\max}-1} s_{q_n}\left(\tau_{\text{RT}}^{(u)}\right)\Phi_{\text{RT}}^{(u)}\Psi_n^{(u)}\right|^2}, \tag{10}$$

assuming complex signals, and $\Phi_{\text{RT}}^{(u)} = \Phi_{\text{FL}}^{(u)}\Phi_{\text{RL}}^{(u)}$ represents the round-trip path loss.

For all following derivations we need to keep in mind that the round-trip noise variance σ_{RT}^2 and the round-trip path loss $\Phi_{\text{RT}}^{(u)}$ depend on $\tau_{\text{RT}}^{(u)}$. After taking the logarithm of (10) and deriving with respect to individual $\tau_{\text{RT}}^{(u)}$ twice, we obtain two Fisher information contributions: the first contribution results from the delay dependent round-trip path loss and thus, relates to a range dependent received signal strength (RSS). As we are not interested in RSS contributions we omit this RSS Fisher information contribution. We focus on the spectral properties of the ranging signal s_q and hence, the second contribution is found to be

$$\left[\text{FIM}\left(\boldsymbol{\tau}_{\text{RT}}\left(\mathbf{r}_q\right)\right)\right]_{u,u} = \frac{2}{\sigma_{\text{RT}}^2}\sum_{n=0}^{N-1}\left|\frac{\partial}{\partial\tau_{\text{RT}}^{(u)}}\sum_{u=1}^{U_{\max}-1} s_{q_n}\left(\tau_{\text{RT}}^{(u)}\right)\Phi_{\text{RT}}^{(u)}\Psi_n^{(u)}\right|^2. \tag{11}$$

From (6) we see that a lower variance requires a larger Fisher information. Consequently, we discuss the result in (11) for modulation independent ranging signals s_q next, as we seek to maximize the Fisher information. At first, we observe the inverse of the round-trip noise σ_{RT}^2 defined in (9). This noise term holds all amplified noise contributions of all relays, attenuated through the delay dependent RL path loss, and the ranging initiator's receiver noise. Ranging precision will therefore depend on the spatial distribution of relays relative to the ranging initiator, the number of relays, and their individual amplification $b^{(u)}$. Next, we observe the sum over N samples of the time-domain ranging signal. A longer observation duration will result in an increased Fisher information. The last part holds the derivative with respect to the desired RTD of the superimposed received ranging signal s_q. A larger derivative in time-domain results in an increased Fisher information. As a consequence, a larger derivative in time-domain requires a signal with higher frequency components and hence, a signal with higher bandwidth. Thus, wideband signals are in general preferred for precise ranging [11], [43].

Finally, we replace the complex ranging signal $s_{q_n}\left(\tau_{\text{RT}}^{(u)}\right)$ with an OFDM modulated signal. With the sampling time T_s we denote the sampled and delayed OFDM signal of length N as

$$s_q\left[nT_s - \tau_{\text{RT}}^{(u)}\right] = \frac{1}{\sqrt{N}}\sum_{l=-N/2}^{N/2-1} S_l e^{\text{j}2\pi l\left(nT_s-\tau_{\text{RT}}^{(u)}\right)}, \tag{12}$$

with the discrete sampling index n. N represents the OFDM symbol length in time-domain without the cyclic prefix and hence, also the number of subcarriers. The sampling time is furthermore denoted as $T_s = 1/f_s = 1/\left(Nf_{\text{sc}}\right)$, with f_{sc} as subcarrier spacing, and $S_l \in \mathbb{C}$ represents a complex number mapped to a specific subcarrier l, e.g., a quadrature amplitude modulation (QAM) data / code symbol. Inserting (12) into (11) and deriving with respect to $\tau_{\text{RT}}^{(u)}$ leads to the lower bound for the variance of a particular range estimate to relay node u of

$$\text{Var}\left\{\hat{d}^{(u)}\left(\mathbf{r}_q\right)\right\} = \frac{c_0^2}{4}\left[\text{Cov}\left\{\hat{\boldsymbol{\tau}}_{\text{RT}}\left(\mathbf{r}_q\right)\right\}\right]_{u,u} \geq \frac{c_0^2}{4}\underbrace{\frac{1}{\frac{8\left(b^{(u)}\pi f_{\text{sc}}\Phi_{\text{RT}}^{(u)}\right)^2}{\sigma_{\text{RT}}^2}\sum_{l=-N/2}^{N/2-1}|S_l|^2\left(\left(l+\varrho^{(u)}\right)\bmod N\right)^2}}_{\text{Fisher information in denominator}}, \tag{13}$$

from which we observe the following interesting aspects: the OFDM symbol's subcarrier spacing f_{sc} appears in the nominator of the Fisher information. Keeping the amount of subcarriers N constant and increasing the subcarrier spacing results in a larger signal bandwidth and subsequently in a larger Fisher information. Subcarrier-mapped QAM symbols S_l appear as absolute values. Hence, ranging variance does not depend on specific phase values mapped on subcarriers l and solely depends on the power we spent for a specific subcarrier l. The unique subcarrier shift $\varrho^{(u)}$ within the modulation term $\Psi^{(u)}$ in (3) appears as cyclic shift in frequency domain, as $\varrho^{(u)}$ is an integer multiple of the subcarrier spacing. The modulo operator is required to reflect the aliasing case, as described previously. Additionally, the subcarrier index appears in its quadratic form. Thus, by allocating subcarriers with higher indices, which inherently lie at the bandwidth edges, the Fisher information can be increased significantly. Furthermore, we can also see from (13) that only the cyclically shifted and observed ranging signal at the ranging initiator's receiver appears in the CRLB and not the initially transmitted ranging signal. Based on this knowledge, a ranging initiator could adapt the transmitted signal to reach particular ranging precision requirements without notifying users operating as relays.

As a next step we evaluate the CRLB from (13) for particular ranging links and swarm formations, based on 3GPP-LTE OFDM PHY-layer parameters. We explicitly chose 3GPP-LTE system parameters to highlight obtained ranging precisions based on signals with medium bandwidth, and to provide comparable results within the wireless communication community.

V. CRLB EVALUATION RESULTS

A. Swarm formations

Before we evaluate the derived CRLB we need to consider different spatial distributions of the cooperative wireless sensor network (WSN). We refer to particular spatial distributions simply as swarm formation. Random swarm formations are arguable to obtain overall range estimation and position estimation performance statistics. However, random swarm formations are not suitable in our case to investigate ranging

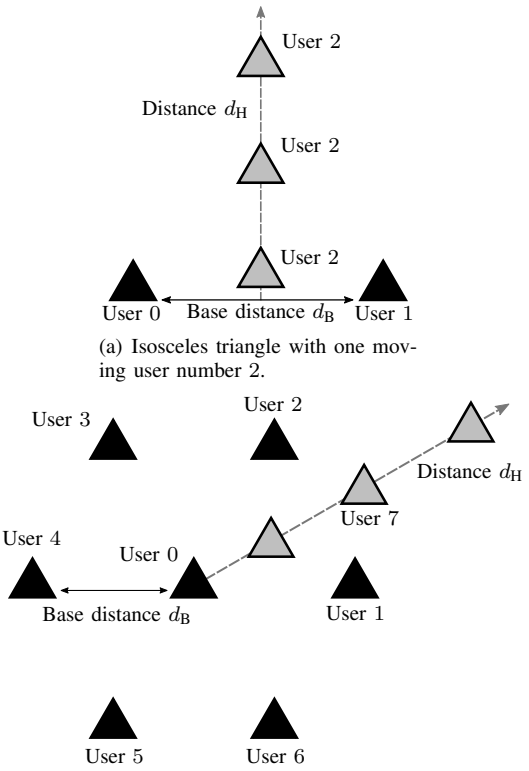

(a) Isosceles triangle with one moving user number 2.

(b) Hexagonal constellation with one moving user number 7.

Fig. 5. Examples of two beneficial swarm formations evaluated in this work.

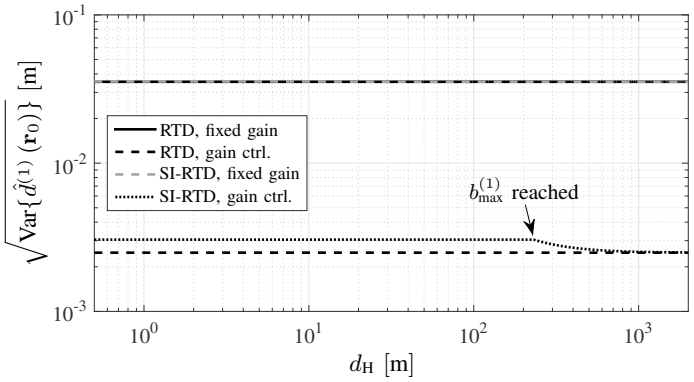

Fig. 6. CRLB evaluation result for swarm formation $\mathrm{F_{Tri}}$ with $d_{\mathrm{B}} = 40\,\mathrm{m}$ for sequential RTD and SI-RTD ranging with fixed gain and gain control (ctrl.). The link between user 0 and user 1 is shown, with ranging initiator $q = 0$ and relay $u = 1$.

precision predicted by the CRLB in detail. Consequently, we focus on two particular two-dimensional swarm formations depicted in Fig. 5. These two swarm formations are basic building blocks to allow for distributed apertures formed by a robotic swarm, and to improve positioning accuracy in a later step. An example of a distributed aperture for a so called return-to-base navigation is investigated in [44]. Other examples showing the benefit of quasi-lattice swarm formation structures for localization and jointly with swarm control over random swarm formations are investigated in [45], [46].

The first swarm formation is an isosceles triangle illustrated in Fig. 5(a) comprising three users. User 0 and user 1 form the triangle base with a fixed base distance denoted as d_{B}. User 2 is located between user 0 and 1 and moves away perpendicular with distance d_{H} to the base. The second swarm formation comprises eight users, with seven users forming a hexagon with one center node, and the eighth user moves away from the center user at an angle of 30°. A base length d_{B} defines the fundamental hexagon size, and the distance between user 0 and the moving user 7 is denoted as d_{H}. Throughout the rest of this article, we refer to the first swarm formation as $\mathrm{F_{Tri}}$ and the hexagon formation as $\mathrm{F_{Hex}}$.

B. Simulation parameters

We evaluate the CRLB with the following simulation parameters: the carrier frequency f_{c} is $5.8\,\mathrm{GHz}$ to reflect a chosen carrier frequency as used in vehicular communications. Channel path loss exponent γ is 2 for free-space transmission, and the propagation speed of light in air is set to $c_0 = 2.9971 \times 10^8\,\mathrm{m\,s^{-1}}$. As we focus on 3GPP-LTE system parameters, we choose a subcarrier spacing f_{sc} of $15\,\mathrm{kHz}$, an OFDM symbol duration without the cyclic prefix of $N = 2048$ samples, and a resulting sampling rate $1/T_s = N f_{\mathrm{sc}} = 30.72\,\mathrm{MHz}$. The allocated bandwidth is 1200 subcarriers, which results in effectively $18\,\mathrm{MHz}$ of bandwidth which is allocable in 3GPP-LTE without carrier aggregation [19], [21]. Unique subcarrier shifts $\varrho^{(u)}$ for each user are assigned as follows: user 0 shifts with zero subcarriers, user 1 with one subcarrier, and so on. For each receiver we assume thermal noise and an additional realistic noise figure NF of $7\,\mathrm{dB}$. Subsequently, the ranging initiator's and relays' noise variances are

$$\sigma_q^2 = \sigma^{2,(u)} = k_{\mathrm{B}} T B \cdot 10^{\frac{\mathrm{NF}}{10}}, \tag{14}$$

with $k_{\mathrm{B}} = 1.380\,65 \times 10^{-23}\,\mathrm{J\,K^{-1}}$ as Boltzmann constant, $T = 300\,\mathrm{K}$ as receiver temperature at $27\,^{\circ}\mathrm{C}$, and $B = 1/T_s$ as receiver noise bandwidth. Mean transmission power is $100\,\mathrm{mW}$ for the chosen carrier frequency. The gain factor $b^{(u)}$ within each relay is set according to two different relaying options: the first option assumes a relay without gain control and hence, we choose a fixed gain $b_{\min}^{(u)} = 53.7\,\mathrm{dB}$ to compensate the FL path loss at a distance of $2\,\mathrm{m}$ for our simulation parameters. The second option assumes a smart relay with gain control to adaptively compensate the FL path loss up to $b_{\max}^{(u)} = 95\,\mathrm{dB}$.

C. Numerical results for the triangular swarm formation

Fig. 6 shows CRLB evaluation results for the static base link of formation $\mathrm{F_{Tri}}$ over increasing distance d_{H}. For comparison we evaluated sequential RTD ranging as state of the art, and our proposed SI-RTD ranging with a sparsity of 3. Every third subcarrier is hence allocated for the broadcasted ranging signal, see Fig. 3. A base distance d_{B} of $40\,\mathrm{m}$ is chosen. The predicted ranging standard deviation is about $3.6\,\mathrm{cm}$ for the fixed gain relaying option. Ranging precision differences between sequential RTD and SI-RTD are negligible. For the adaptive gain control option we clearly observe a difference: in case of sequential RTD we obtain a ranging precision of

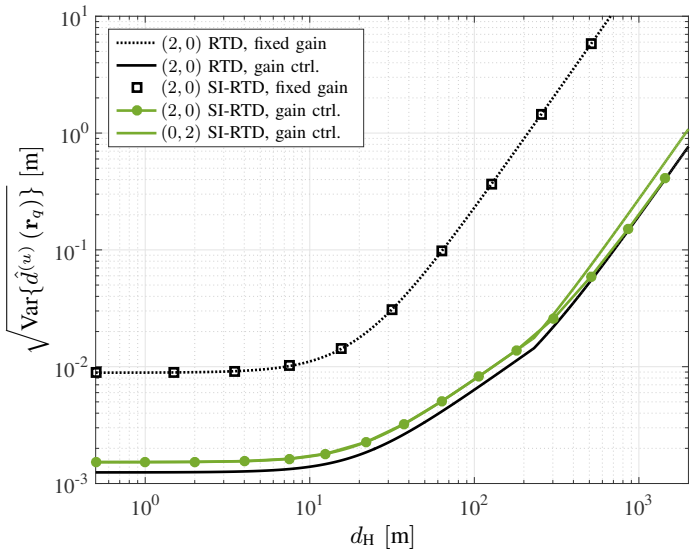

Fig. 7. CRLB evaluation result for swarm formation $\mathrm{F_{Tri}}$ with $d_\mathrm{B} = 40\,\mathrm{m}$ for sequential RTD and SI-RTD ranging with fixed gain and gain control (ctrl.). The link between the moving user 2 and the static user 0 is shown. The tuple (q, u) denotes a link combination with ranging initiator q and relay u.

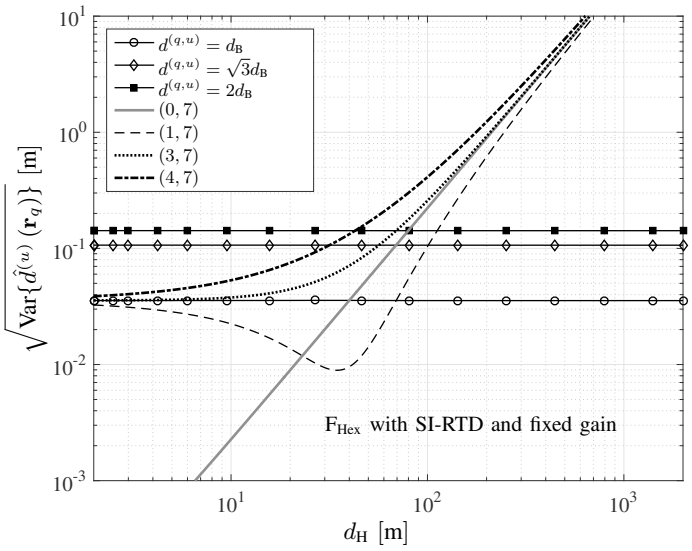

Fig. 8. CRLB evaluation result for swarm formation $\mathrm{F_{Hex}}$ with base distance $d_\mathrm{B} = 40\,\mathrm{m}$ for SI-RTD based ranging with fixed gain.

about $2.5\,\mathrm{mm}$, which remains constant over d_H. In case of our proposed SI-RTD we obtain a ranging precision of about $3\,\mathrm{mm}$. This precision decrease is expected, as the relayed noise from user 2 in Fig. 5(a) significantly contributes to the joint noise term in (9) due to the adaptive gain control. However, the resulting precision degradation compared to RTD is only $20\,\%$. From Fig. 6 we also observe a bend for SI-RTD with the gain control option at $d_\mathrm{H} \approx 240\,\mathrm{m}$. This bend results from the moving user 2 reaching the adaptive gain limit of $b_\mathrm{max}^{(u)} = 95\,\mathrm{dB}$. The user 2 relay gain is therefore fixed for d_H above $240\,\mathrm{m}$. As a result, user 2's noise contribution becomes smaller for increased d_H and the predicted ranging precision of SI-RTD approaches sequential RTD. An additional investigation into user 0 and user 1 link combinations showed a negligible difference for this static link, and we can state $\mathrm{Var}\{\hat{d}^{(1)}(\mathbf{r}_0)\} \approx \mathrm{Var}\{\hat{d}^{(0)}(\mathbf{r}_1)\}$.

Next, we are interested in predicted ranging precisions for the dynamic link between moving user 2 and static users 0 and 1 of swarm formation $\mathrm{F_{Tri}}$. As introduced in Fig. 1, we denote a specific link combination between a ranging initiator q and a relay u as tuple (q, u). Fig. 7 shows results for dynamic links, and we focus on sequential RTD and SI-RTD with fixed gain first. Observable ranging precision differences between RTD and SI-RTD are negligible: for $d_\mathrm{H} = 0\,\mathrm{m}$ the range to the static nodes is $20\,\mathrm{m}$ and hence, the resulting predicted precision is about $0.9\,\mathrm{cm}$. The forward link path loss is not compensated and the predicted ranging standard deviation significantly increases with d_H. At $d_\mathrm{H} = 100\,\mathrm{m}$ the predicted ranging precision is about $23\,\mathrm{cm}$. A ranging precision of $23\,\mathrm{m}$ is obtained at $d_\mathrm{H} = 1\,\mathrm{km}$, which is unfavorable for precise swarm formation estimation. Consequently, relaying users with gain control should be considered, for which results are shown in Fig. 7. We focus on link combination $(2, 0)$ first, and clearly see a lower ranging standard deviation for RTD, as well as SI-RTD. The gap between RTD and SI-RTD is comparable to the observable gap in Fig. 6, and the bend at $d_\mathrm{H} \approx 240\,\mathrm{m}$ again results from reaching the adaptive gain limit within the relay. For $d_\mathrm{H} = 1\,\mathrm{km}$ we obtain a ranging precision of about $27\,\mathrm{cm}$ compared to the fixed gain option for which we obtained $23\,\mathrm{m}$. Ranging link combinations $(2, 0)$ and $(0, 2)$ show one interesting aspect, see Fig. 7: in case where user 2 is the ranging initiator q we observe that the ranging precision obtained through SI-RTD approaches the ranging precision obtained by sequential RTD for larger d_H. This results from the fact that in case where user 2 is the ranging initiator, the ranging links $(2, 0)$ and $(2, 1)$ are equally balanced, and relayed noise of user 1 contributes lesser above the gain control limit. In case where, for example, user 0 is the ranging initiator, there is always a stronger noise contribution from the static user 1 which dominates the overall noise term, see (9).

This first CRLB evaluation for swarm formation $\mathrm{F_{Tri}}$ illustrated in Fig. 5(a) shows that we obtain a slightly worse ranging precision of about $20\,\%$ based on our proposed SI-RTD concept compared to state of the art sequential RTD. However, we obtain a factor of $U_\mathrm{max} - 1 = 2$ higher ranging link evaluation update rate compared to state of the art for swarm formation $\mathrm{F_{Tri}}$. As a result, we trade a minor precision decrease with a much higher update rate. Predicted ranging precisions with 3GPP-LTE system parameters and with adaptive gain control are favorable for precise swarm formation estimation.

D. Numerical results for the hexagonal swarm formation

The second evaluated swarm formation is $\mathrm{F_{Hex}}$ illustrated in Fig. 5(b), with a base distance d_B of $40\,\mathrm{m}$. A sparsity of 8 is chosen, and hence, only every eighth OFDM subcarrier is allocated for the ranging signal emitted by a ranging initiator. For formation $\mathrm{F_{Hex}}$ with its eight users we obtain $U_\mathrm{max}\,(U_\mathrm{max} - 1) = 56$ individual ranging links. As this hexagonal formation has symmetries, we group ranging links for better visualization. At first, we focus on SI-RTD and

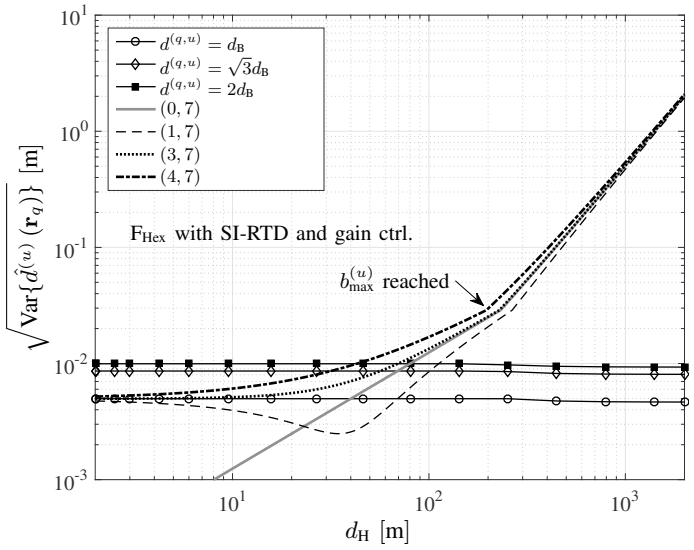

Fig. 9. CRLB evaluation result for swarm formation $\mathrm{F_{Hex}}$ with base distance $d_\mathrm{B} = 40\,\mathrm{m}$ for SI-RTD based ranging with gain control.

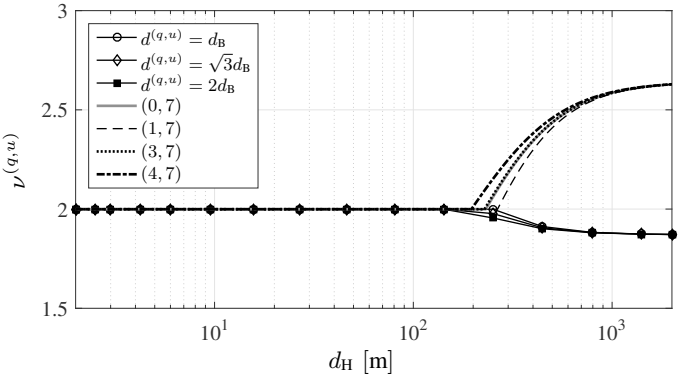

Fig. 10. Ranging standard deviation degradation factor $\nu^{(q,u)}$, see (15) of the proposed SI-RTD ranging scheme compared to state of the art sequential RTD ranging.

RTD with fixed gain relays. Fig. 8 shows predicted ranging precisions. Ranging links between static users are grouped into three different groups: one group for distances of d_B as between user 0 and 4, one group for distances of $\sqrt{3}d_\mathrm{B}$ as between user 3 and 5, and one group for distances of $2d_\mathrm{B}$ as between user 2 and 5. Each group holds 24, 12, and 6 specific links respectively. In Fig. 8 we observe a precision of $3.6\,\mathrm{cm}$ for link groups $d^{(q,u)} = d_\mathrm{B}$, and a precision of $14.2\,\mathrm{cm}$ for link groups $d^{(q,u)} = 2d_\mathrm{B}$. Dynamic links are grouped into four distinct groups $(0, 7)$, $(1, 7)$, $(3, 7)$, $(4, 7)$, and we clearly see the increasing ranging standard deviation over d_H. The predicted ranging precision is about $24\,\mathrm{m}$ at $d_\mathrm{H} = 1\,\mathrm{km}$. For link $(1, 7)$ we observe an improving ranging precision at small d_H, resulting from user 7 being located at the closest proximity to static users 2 and 1. A further investigation revealed negligible differences between RTD and SI-RTD ranging for relays with fixed gain settings. Hence, results for state of the art RTD ranging are omitted.

Fig. 9 shows CRLB evaluation results for SI-RTD based ranging as in Fig. 8 but with gain control in each relay. A significant ranging precision improvement is obtained: for the three grouped static link combinations we obtain predicted ranging precisions between $0.5\,\mathrm{cm}$ and $1\,\mathrm{cm}$. The standard deviation at $d_\mathrm{H} = 1\,\mathrm{km}$ reduces from $24\,\mathrm{m}$ in the fixed gain case to $0.54\,\mathrm{m}$ in the gain control case. Once the gain control reaches the limit of $b^{(u)}_{\max}$ at d_H between $200\,\mathrm{m}$ and $260\,\mathrm{m}$, the predicted ranging precision degrades significantly. Nevertheless, predicted ranging precisions appear favorable for precise robotic swarm formation estimation.

E. Comparison between RTD and SI-RTD

For our last investigation we compare predicted ranging precisions based on RTD and SI-RTD for swarm formation $\mathrm{F_{Hex}}$. Based on observations of swarm formation $\mathrm{F_{Tri}}$ in Fig. 6 and Fig. 7 we already know that we trade a minor precision decrease with SI-RTD based ranging compared to RTD at the benefit of much higher update rates. We denote a ranging precision degradation factor $\nu^{(q,u)}$ as

$$\nu^{(q,u)} = \frac{\sqrt{\mathrm{Var}_{\text{SI-RTD}}\{\hat{d}^{(u)}(\mathbf{r}_q)\}}}{\sqrt{\mathrm{Var}_{\text{RTD}}\{\hat{d}^{(u)}(\mathbf{r}_q)\}}}, \tag{15}$$

which relates the precision of SI-RTD and RTD based ranging. Fig. 10 shows $\nu^{(q,u)}$ for swarm formation $\mathrm{F_{Hex}}$ over traveled user 7 distance d_H. Relaying users apply gain control. We observe two interesting aspects: firstly, as long as the maximum gain is not reached the degradation factor is $\nu^{(q,u)} = 2$. Secondly, beyond the maximum gain limit we see an increasing degradation factor for all dynamic links, which converges to a limit of about 2.6. The precision degradation becomes smaller beyond the maximum gain limit for static links, and converges to a limit of about 1.9. Investigating these two limits revealed an upper degradation limit for the dynamic links of $\sqrt{U_{\max} - 1} = \sqrt{7} \approx 2.65$ and a lower degradation limit for the static links of $\sqrt{(U_{\max} - 1)/2} \approx 1.87$.

VI. Conclusion

As a conclusion we can state that ranging precisions predicted by the derived CRLB are very favorable for precise robotic swarm formation estimation, particularly for robotic swarms with high relative mobility. A bandwidth of $18\,\mathrm{MHz}$ as used in 3GPP-LTE is sufficient to achieve high ranging precisions in uncluttered environments. Our proposed subcarrier-interleaved orthogonal multi-user access allows significantly higher ranging update rates compared to state of the art and linearly scales with the number of users in a cooperative wireless sensor network, compared to a quadratic scaling of state of the art access schemes. Furthermore, our joint view on the physical layer and MAC layer enables a system design with a trade-off between a minor precision decrease and a much higher update rate.

Acknowledgment

This work has been performed in the framework of the German Aerospace Center (DLR) project *Dependable Navigation*.

REFERENCES

[1] S. Sand, S. Zhang, M. Mühlegg, G. Falconi, C. Zhu, T. Krüger, and S. Nowak, "Swarm Exploration and Navigation on Mars," in *International Conference on Localization and GNSS (ICL-GNSS)*, Jun. 2013, pp. 1 – 6.

[2] A. Viseras Ruiz, M. Angermann, I. Wieser, M. Frassl, and J. üller, "Efficient Multi-Agent Exploration with Gaussian Processes," in *Australasian Conference on Robotics and Automation (ACRA)*, Melbourne, Australia, Dec. 2014.

[3] A. Viseras Ruiz and C. Olariu, "A General Algorithm for Exploration with Gaussian Processes in Complex, Unknown Environments," in *IEEE International Conference on Robotics and Automation (ICRA)*, Seattle, USA, May 2015, pp. 3388 – 3393.

[4] B. J. Julian, M. Angermann, M. Frassl, and M. Lichtenstern, "Towards a Unifying Information Theoretic Framework for Multi-Robot Exploration and Surveillance," in *Robotics: Science and Systems - Workshop*, Los Angeles, CA, USA, Jun. 2011.

[5] F. Gustafsson and F. Gunnarsson, "Mobile Positioning Using Wireless Networks: Possibilities and fundamental limitations based on available wireless network measurements," *IEEE Signal Process. Mag.*, vol. 22, no. 4, pp. 41 – 53, Jul. 2005.

[6] N. Patwari, J. Ash, S. Kyperountas, A. Hero, R. Moses, and N. Correal, "Locating the Nodes: Cooperative localization in wireless sensor networks," *IEEE Signal Process. Mag.*, vol. 22, no. 4, pp. 54 – 69, Jul. 2005.

[7] H. Wymeersch, J. Lien, and M. Win, "Cooperative Localization in Wireless Networks," *Proc. IEEE*, vol. 97, no. 2, pp. 427 – 450, Feb. 2009.

[8] H.-Y. Huang, A. Khendry, and T. G. Robertazzi, "Layernet: A Self-Organizing Protocol for Small Ad Hoc Networks," *IEEE Trans. Aerosp. Electron. Syst.*, vol. 38, no. 2, pp. 378 – 387, Apr. 2002.

[9] M. Hadded, P. Muhlethaler, A. Laouiti, R. Zagrouba, and L. Saidane, "TDMA-Based MAC Protocols for Vehicular Ad Hoc Networks: A Survey, Qualitative Analysis, and Open Research Issues," *Communications Surveys Tutorials, IEEE*, vol. 17, no. 4, pp. 2461 – 2492, Fourth quarter 2015.

[10] I.-S. S. Board, "Part 11: Wireless LAN Medium Access Control (MAC) and Physical Layer (PHY) Specifications," The Institute of Electrical and Electronics Engineers, Inc., Tech. Rep., Feb. 2012.

[11] D. Dardari, A. Conti, U. Ferner, A. Giorgetti, and M. Win, "Ranging With Ultrawide Bandwidth Signals in Multipath Environments," *Proc. IEEE*, vol. 97, no. 2, pp. 404 – 426, Feb. 2009.

[12] H. Jang, E. Kim, J.-J. Lee, and J. Lim, "Location-Based TDMA MAC for Reliable Aeronautical Communications," *IEEE Trans. Aerosp. Electron. Syst.*, vol. 48, no. 2, pp. 1848 – 1854, Apr. 2012.

[13] B. Denis, M. Maman, and L. Ouvry, "On the Scheduling of Ranging and Distributed Positioning Updates in Cooperative IR-UWB Networks," in *Proc. IEEE Int. Conf. Ultra-Wideband*, 2009, pp. 370 – 375.

[14] S. R. Zekavat and R. Buehrer, *Handbook of Position Location: Theory, Practice, and Advances*. Wiley-IEEE Press, 2012.

[15] B. Sheng, "Enhanced OFDM-based ranging method for space applications," *IEEE Trans. Aerosp. Electron. Syst.*, vol. 50, no. 2, pp. 1606 – 1609, Apr. 2014.

[16] G. Ren, C. Sun, H. Ni, and Y. Bai, "OFDM-Based Precise Ranging Technique in Space Applications," *IEEE Trans. Aerosp. Electron. Syst.*, vol. 47, no. 3, pp. 2217 – 2221, Jul. 2011.

[17] Y.-H. Jung, S. Cho, and C. You, "Decentralised ranging method for orthogonal frequency division multiplex access systems with amplify-and-forward relays," *IET Communications*, vol. 8, no. 9, pp. 1609 – 1615, Feb. 2014.

[18] P. Ferrari, A. Flammini, E. Sisinni, A. Depari, M. Rizzi, R. Exel, and T. Sauter, "Timestamping and Ranging Performance for IEEE 802.15.4 CSS Systems," *IEEE Trans. Instrum. Meas.*, vol. 63, no. 5, pp. 1244 – 1252, May 2014.

[19] G. O. Partners, "LTE; Evolved Universal Terrestrial Radio Access (E-UTRA); Physical channels and modulation (3GPP TS 36.211 version 8.7.0 Release 8)," European Telecommunications Standards Institute (ETSI), Tech. Rep., 2009.

[20] M. Müller, "IEEE 802.16m Technology Introduction," Rohde & Schwarz, Tech. Rep., Jul. 2010.

[21] S. Sesia, I. Toufik, and M. Baker, *LTE - The UMTS Long Term Evolution: From Theory to Practice*. John Wiley & Sons Ltd, 2009.

[22] G. Lellouch, A. K. Mishra, and M. Inggs, "Stepped OFDM Radar Technique to Resolve Range and Doppler Simultaneously," *IEEE Trans. Aerosp. Electron. Syst.*, vol. 51, no. 2, pp. 937 – 950, Apr. 2015.

[23] R. F. Tigrek, W. J. A. D. Heij, and P. V. Genderen, "OFDM Signals as the Radar Waveform to Solve Doppler Ambiguity," *IEEE Trans. Aerosp. Electron. Syst.*, vol. 48, no. 1, pp. 130 – 143, Jan. 2012.

[24] S. C. Surender and R. M. Narayanan, "UWB Noise-OFDM Netted Radar: Physical Layer Design and Analysis," *IEEE Trans. Aerosp. Electron. Syst.*, vol. 47, no. 2, pp. 1380 – 1400, Apr. 2011.

[25] K. Kauffman, J. Raquet, Y. Morton, and D. Garmatyuk, "Real-Time UWB-OFDM Radar-Based Navigation in Unknown Terrain," *IEEE Trans. Aerosp. Electron. Syst.*, vol. 49, no. 3, pp. 1453 – 1466, Jul. 2013.

[26] E. Staudinger, S. Zhang, A. Dammann, and C. Zhu, "Towards a Radio-Based Swarm Navigation System on Mars – Key Technologies and Performance Assessment," in *Proc. IEEE Int. Conf. on Wireless for Space and Extreme Environments (WiSEE)*, Noordwijk, Netherlands, Oct. 2014.

[27] J. Degesys, I. Rose, A. Patel, and R. Nagpal, "DESYNC: Self-Organizing Desynchronization and TDMA on Wireless Sensor Networks," in *6th International Symposium on Information Processing in Sensor Networks*, Apr. 2007, pp. 11 – 20.

[28] R. Pagliari, Y. W. P. Hong, and A. Scaglione, "Pulse coupled oscillators' primitives for collision-free multiple access with application to body area networks," in *First International Symposium on Applied Sciences on Biomedical and Communication Technologies*, Oct. 2008, pp. 1 – 5.

[29] Y. Wang and F. J. Doyle, "Optimal Phase Response Functions for Fast Pulse-Coupled Synchronization in Wireless Sensor Networks," *IEEE Trans. Signal Process.*, vol. 60, no. 10, pp. 5583 – 5588, Oct. 2012.

[30] F. Shin, L. Zhiwei, and L. Xing, "Symmetric Multi-Way Ranging for Wireless Sensor Network," in *Proc. IEEE Int. Symposium on Personal, Indoor and Mobile Radio Communications*, Sep. 2007.

[31] L. Xing, L. Zhiwei, and F. Shin, "Symmetric Double Side Two Way Ranging with Unequal Reply Time," in *Proc. IEEE Vehicular Technology Conf. Fall*, Sep. 2007, pp. 1980 – 1983.

[32] P. Ferrari, A. Flammini, E. Sisinni, A. Depari, M. Rizzi, R. Exel, and T. Sauter, "Timestamping and Ranging Performance for IEEE 802.15.4 CSS Systems," *IEEE Trans. Instrum. Meas.*, vol. 63, no. 5, pp. 1244 – 1252, May 2014.

[33] J. Lee, Z. Lin, P. Chin, and C. Law, "The Use of Symmetric Multi-Way Two Phase Ranging to Compensate Time Drift in Wireless Sensor Network," *IEEE Trans. Wireless Commun.*, vol. 8, no. 2, pp. 613 – 616, Feb. 2009.

[34] E. Staudinger and A. Dammann, "Round-Trip Delay Ranging with OFDM Signals – Performance Evaluation with Outdoor Experiments," in *Proc. IEEE Workshop Positioning Navigation and Communication*, Dresden, Germany, Mar. 2014.

[35] ——, "Round-Trip Delay Indoor Ranging Experiments with OFDM Signals," in *Proc. IEEE Int. Conf. on Communications*, Sydney, Australia, Jun. 2014, pp. 150 – 156.

[36] ——, "Sparse Subcarrier Allocation for Timing-based Ranging with OFDM Modulated Signals in Outdoor Environments," in *Proc. IEEE Workshop Positioning Navigation and Communication*, Dresden, Germany, Mar. 2013.

[37] M. Morelli, C.-C. Kuo, and M.-O. Pun, "Synchronization Techniques for Orthogonal Frequency Division Multiple Access (OFDMA): A Tutorial Review," *Proc. IEEE*, vol. 95, no. 7, pp. 1394 – 1427, Jul. 2007.

[38] M. Morelli, L. Sanguinetti, and H. V. Poor, "A robust ranging scheme for ofdma-based networks," *IEEE Trans. Commun.*, vol. 57, no. 8, pp. 2441 – 2452, Aug. 2009.

[39] X. Fu, Y. Li, and H. Minn, "A new ranging method for ofdma systems," *IEEE Trans. Wireless Commun.*, vol. 6, no. 2, pp. 659 – 669, Feb. 2007.

[40] J. Zeng and H. Minn, "A novel ofdma ranging method exploiting multiuser diversity," *IEEE Trans. Commun.*, vol. 58, no. 3, pp. 945 – 955, Mar. 2010.

[41] Z. Wang, F. Tigrek, O. Krasnov, F. V. D. Zwan, P. V. Genderen, and A. Yarovoy, "Interleaved ofdm radar signals for simultaneous polarimetric measurements," *IEEE Trans. Aerosp. Electron. Syst.*, vol. 48, no. 3, pp. 2085 – 2099, Jul. 2012.

[42] S. M. Kay, *Fundamentals of Statistical Processing — Estimation Theory*. Prentice Hall, 1993.

[43] S. Gezici, Z. Tian, G. B. Giannakis, H. Kobayashi, A. F. Molisch, H. V. Poor, and Z. Sahinoglu, "Localization via Ultra-Wideband Radios: A look at positioning aspects for future sensor networks," *IEEE Signal Process. Mag.*, vol. 22, no. 4, pp. 70 – 84, Jul. 2005.

[44] C. Zhu, S. Zhang, A. Dammann, S. Sand, P. Henkel, and C. Günther, "Return-to-Base Navigation of Robotic Swarms in Mars Exploration Using DoA Estimation," in *Proceedings of* 55^{th} *International Symposium ELMAR 2013*, Zadar, Croatia, Sep. 2013.

[45] S. Zhang, E. Staudinger, S. Sand, R. Raulefs, and A. Dammann, "Anchor-Free Localization using Round-Trip Delay Measurements for Martian Swarm Exploration," in *Proc. The Institute of Navigation (ION) Position Location and Navigation Symposium (PLANS)*, Monterey, California, USA, May 2014.

[46] S. Zhang and R. Raulefs, "Multi-Agent Flocking with Noisy Anchor-Free Localization," in *Wireless Communications Systems (ISWCS), 2014 11th International Symposium on*. IEEE, 2014, pp. 927 – 933.

Emanuel Staudinger received the M.Sc. degree in Embedded Systems Design from the University of Applied Sciences of Hagenberg, Austria, in 2010. Since 2010, he is with the Institute of Communications and Navigation of the German Aerospace Center (DLR), Wessling, Germany. He received the Ph.D. degree at the Institute of Electrodynamics and Microelectronics of the University of Bremen in 2015. His research interests and activities include ranging signal design for cooperative positioning, rapid-prototyping of measurement test-beds, measurements outdoors and indoors, and analyzing measurements for cross-validation with lower bounds.

Siwei Zhang obtained his M.Sc. degree in communications engineering from the Technical University of Munich (TUM), Germany, in 2011. Since 2012, he is working with the German Aerospace Center (DLR) as a researcher. His research interests include statistical signal processing for radio navigation, particularly for cooperative localization, relative localization/tracking and swarm navigation.

Armin Dammann received the M.Sc. and Ph.D. degrees in electrical engineering from the University of Ulm, Ulm, Germany, in 1997 and 2005, respectively. In 1997, he joined the Institute of Communications and Navigation, German Aerospace Center (DLR), Wessling, Germany, where he has been the Head of the Mobile Radio Transmission Research Group since 2005. His research interests and activities include signal design and signal processing for wireless communication and navigation systems. He has been active in several European Union projects, e.g., WINNER, WHERE, and WHERE2.